Appl Microbiol Biotechnol (2014) 98:4975–4985
DOI 10.1007/s00253-013-5505-6

Directed evolution of nitrobenzene dioxygenase for the synthesis of the antioxidant hydroxytyrosol

Kalia Bernath-Levin · Janna Shainsky · Liron Sigawi · Ayelet Fishman

Received: 14 October 2013 / Revised: 20 December 2013 / Accepted: 26 December 2013 / Published online: 25 January 2014

Abstract Nitrobenzene dioxygenase (NBDO) is known to add both atoms of molecular oxygen to the aromatic ring of nitrobenzene to form catechol. It is assembled by four subunits of which the alpha subunit is responsible for catalysis. As an oxidizing enzyme, it has a potential use in the detoxification of industrial waste and the synthesis of pharmaceuticals and food ingredients; however, not much work has been done studying its structure-function correlations. We used several protein engineering approaches (neutral drift libraries, random libraries, two types of focused libraries, and family shuffling) to engineer NBDO for the production of the highly potent antioxidant, hydroxytyrosol (HTyr), from the substrate 3-nitrophenethyl alcohol (3NPA). We obtained a triple mutant, F222C/F251L/G253D, which is able to oxidize 3NPA 375-fold better than wild type with a very high regioselectivity. In total, we identified four positions which are important for acquisition of new specificities, of which only one is well-known and studied. Based on homology modeling, it is suggested that these mutations increase activity by vacating extra space within the active site for the larger substrate and also by hydrogen bonding to the substrate. The best variant had acquired a stabilizing mutation which was beneficial only in this mutant. Thus, we have achieved two goals, the first is the enzymatic production of HTyr, and the second is valuable information regarding the structure-function correlations of NBDO.

Keywords Nitrobenzene dioxygenase · Hydroxytyrosol · Protein engineering · Neutral drift · Family shuffling

Introduction

Oxidizing enzymes have considerable industrial potential, since they are able to add an oxygen molecule to industrially important compounds such as substituted aromatics. However, their full potential has not been exploited due to their complexity: They have several subunits and require regeneration of the reducing cofactor (Friemann et al. 2005). Nitrobenzene dioxygenase (NBDO) is assembled by a reductase, a ferredoxin, and an oxygenase having an $\alpha_3\beta_3$ quaternary structure. It belongs to the Rieske nonheme iron dioxygenase family and is known to add both atoms of molecular oxygen to the aromatic ring of nitrobenzene while liberating nitrite to form catechol (Kovaleva and Lipscomb 2008). The enzyme was found in bacteria (*Pseudomonas pseudoalcaligenes* JS45) isolated from nitrobenzene-contaminated industrial facility; it appears to have evolved the nitrobenzene-degradation ability quite recently (Ju and Parales 2011; Parales et al. 2005).

One of our goals was to use protein engineering and directed evolution methods to modulate NBDO and isolate variants which are able to produce hydroxytyrosol (HTyr), a highly potent natural antioxidant, from an inexpensive substrate, 3-nitrophenethyl alcohol (3NPA; Fig. 1). Much work has been published on the qualities of this antioxidant, for example, anticancer, antiatherogenic, and antibacterial activities (Bouallagui et al. 2011; Cicerale et al. 2012). Routinely, HTyr is produced from organic parts of the olive fruit and from waste streams (Allouche et al. 2003); however, this is quite a laborious and polluting process with varying yields (Allouche et al. 2003). In addition, enzymatic methods have been published for producing HTyr from tyrosol by whole

Electronic supplementary material The online version of this article (doi:10.1007/s00253-013-5505-6) contains supplementary material, which is available to authorized users.

K. Bernath-Levin · J. Shainsky · L. Sigawi · A. Fishman (✉)
Department of Biotechnology and Food Engineering,
Technion-Israel Institute of Technology, Haifa 32000, Israel
e-mail: afishman@tx.technion.ac.il

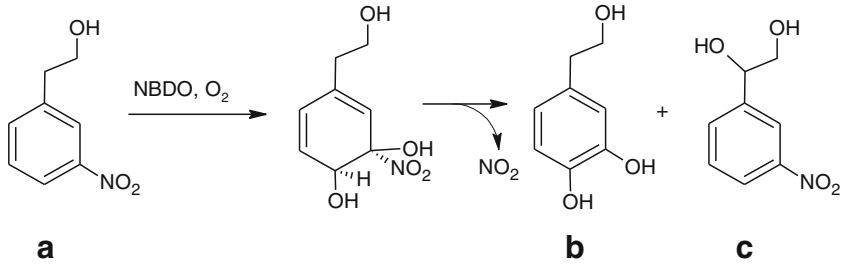

Fig. 1 Dioxygenation of **a** 3-nitrophenethyl alcohol (3NPA) by NBDO to form **b** hydroxytyrosol (HTyr) or **c** 3-nitrophenyl 1,2-ethanediol

cells or enzymes (Allouche et al. 2004; Allouche and Sayadi 2005; Espin et al. 2001). One method which was based on directed evolution of toluene 4-monooxygenase (T4MO) resulted in a triple variant, which could produce HTyr from 2-phenylethanol 190-fold better than wild type (Brouk and Fishman 2009; Brouk et al. 2010). Satoh et al. (2012) recently engineered a metabolic pathway in *Escherichia coli* to produce HTyr from tyrosol or sugar. All these attempts point to the great interest there is in producing natural HTyr by an enzymatic process.

The second goal of this work was to study structure-function correlations of NBDO using various protein engineering tools. As mentioned above, oxygenases are quite complex; however, their industrial use is valuable (Fuchs et al. 2011). Within this group of enzymes, there is limited work on NBDO. Only a few papers were published in which residues in the active site were modulated based on structural analysis and sequence alignment (Ju and Parales 2006; Lessner et al. 2002). The potential of these residues was only partially explored by screening libraries of single-point mutagenesis (Ju and Parales 2006; Shainsky et al. 2013). These studies identified few important residues which affect selectivity and activity of NBDO, with the ratio of oxidation products reversed in reactions with certain nitrotoluenes. Nevertheless, most of the activity changes were either modest or using model substrates. In the present work, we extensively explored NBDO's potential for the synthesis of HTyr using various protein engineering tools: neutral drift libraries, random libraries via error-prone PCR, family shuffling, and focused libraries. We have discovered new mutations and new combinations of mutations, which could not have been discovered by the other methods. These mutations have a dramatic effect on activity (375-fold improvement) and regioselectivity.

Materials and methods

Bacterial strains, cloning, and growth conditions The four genes encoding NBDO were cloned into a pETDuet vector (Novagen ®, Merck KgaA, Darmstadt, Germany), as described earlier (Shainsky et al. 2013), to obtain the pETDuet-Nbz plasmid. The plasmid was transformed into BL21 (DE3) cells (*F^- ompT gal dcm lon hsdS_B(r_B^- m_B^-) λ (DE3 [lacI lacUV5-T7 gene 1 ind1 sam7nin5]*)Novagen ®, Merck KgaA, Darmstadt, Germany) grown in Luria-Bertani (Dalby) medium supplemented with 100-μg/ml ampicillin (LB-amp) (Sambrook et al. 1989). To translate the protein, an overnight culture was prepared by inoculating 2–5-ml LB with a single colony and shaking overnight at 37 °C at 250 rpm on a TU-400 incubator shaker (Orbital shaker incubator, MRC, Holon, Israel). Fresh LB-amp media was inoculated at a 1:100 or 1:50 ratio with the overnight culture and grown at 37 °C, with shaking, to optical density of OD_{600}= 0.4–0.6. At this point, 0.5-mM isopropyl β-D-1-thiogalactopyranoside (IPTG) was added, and the cells were transferred to 30 °C for additional 2-h shaking.

Whole cell enzymatic biotransformation Cells expressing the various mutant or wild type genes were grown in 120-ml LB as described above. At the end of cell growth, after protein translation, the cells were centrifuged at 8,000×*g* for 10 min with a 12256 rotor of Sigma-4K15 centrifuge (Sigma, Osterode, Germany) and resuspended in 100-mM potassium phosphate buffer at pH 7 to OD_{600}=10. The substrate, 3-nitrophenethyl alcohol (3NPA, Santa-Cruz Biotechnology, USA), or nitrobenzenes (NB, Sigma-Aldrich Chemicals Ltd., Rehovot, Israel) were added at a final concentration of 0.5 mM, and the cells were shaken at 30 °C in a flask. At various time points, 1-ml sample was collected from the flask into a 1.5-ml tube. Normally, samples were collected at 1, 2, 3, 4, 5, 6, 10, 15, and 30 min for a fast reacting mutant (Fig. S4). The sample was centrifuged and the supernatant stored on ice for further analyses. Analysis of reaction rate was done by the NO_2 release assay (Ju and Parales 2006), whereas the reaction products were analyzed by reverse-phase high-performance liquid chromatography (HPLC), gas chromatography coupled to mass spectrometry (GC-MS), and nuclear magnetic resonance (NMR). Results represent at least three replicates.

Plate screening Single colonies from the freshly transformed library were picked into 96-deep well plates containing 300-μl LB-amp and grown overnight at 37 °C with shaking. The overnight culture was used to inoculate 1-ml LB-amp dispensed in fresh deep well plates at a 1:50 ratio, using a

multichannel pipette. The bacteria were grown at 37 °C to OD_{600}≈0.4–0.6, then 0.5-mM IPTG was added, and the bacteria were transferred to 30 °C for 2 h for protein translation. Next, the deep well plates were centrifuged using a 11144/13145 rotor of Sigma-4K15 centrifuge (Sigma, Osterode, Germany), and cell pellet was resuspended in 200 μl (for screens on NB as substrate) or 150 μl (for screens on 3NPA as substrate) of 100-mM potassium phosphate buffer pH 7 containing 0.5 mM of the chosen substrate. The plates with the resuspended bacteria were incubated with shaking at 30 °C either overnight (in case of NB screens and round 1–round 2 screens) or for shorter time periods (0.5–5 h) in case of screens of the increased activity mutants from the second round of selection (round 2). After incubation, the biotransformation supernatant was separated from the cell pellet by centrifugation. The screen for activity on NB was based on a method for catechol detection (Fishman et al. 2004; Schmidt and Bornscheuer 2005). The biotransformation supernatant of 100 μl was transferred to a 96-well plate, to which 100 μl of 2-mM sodium periodate solution (prepared in water) was added. Color absorbance was detected at 450 nm within 10 min using a multiplate reader (Molecular Devices, Sunny Vale, CA, USA). The screen for activity on 3NPA was done using the NO_2 release assay described below.

NO_2 release assay The assay is based on a method described elsewhere (Ju and Parales 2006). Briefly, 50 μl of the whole cell biotransformation supernatant or a solution of sodium nitrite prepared in buffer was mixed with 50 μl of 1 % sulfanilamide (Sigma-Aldrich Chemicals Ltd., Rehovot, Israel) prepared in 1.5 M HCl in a 96-well plate. After 5-min incubation at room temperature, 50 μl of 0.02 % N-(1-naphtyl) ethylenediamine dihydrochloride (Sigma-Aldrich chemicals Ltd., Rehovot, Israel) prepared in 1.5 M HCl was added. After an additional 5-min incubation at room temperature, the sample was cooled on ice, and color absorbance was measured at 550 nm. The initial velocity of each mutant was calculated as the amount of NO_2 released in nmol min^{-1} mg^{-1} protein at various time points between 0 and 5 h (Brouk and Fishman 2009). To determine the amount of NO_2 released, a calibration curve was prepared from sodium nitrite. The protein content was measured using the Bradford assay (Bradford 1976). For kinetic measurements, an aliquot of 1 ml was removed at various time points during whole cell biotransformation (after addition of the substrate). The aliquot was immediately centrifuged and the supernatant analyzed by the NO_2 release assay (see above). The quantity of nitrite released was divided by the protein content in each 1-ml biotransformation sample to give the specific activity in nmol NO_2 min^{-1} mg $protein^{-1}$. The protein content of whole cells expressing the NBDO genes was measured by the Bradford analysis. The initial velocity was determined based on at least five time points.

Library construction and site-directed mutagenesis Random mutagenesis was performed using the GeneMorph II random mutagenesis kit (Agilent Technologies, Santa Clara, CA, USA) according to the manufacturer's instructions. The mutagenesis level was modulated by changing the template concentration and number of PCR cycles. Mutagenesis rate was determined by sequencing 10–12 random colonies of the amplified library. The best mutagenesis level (~3 mutations/gene) was achieved by amplifying 340-ng template in a 25-μl PCR reaction using 14 cycles. This PCR product was further amplified with a proofreading taq polymerase (Phusion taq, New England BioLabs Inc, USA) and cloned into a pETDuet plasmid, which contained the ferredoxin, reductase, and β-oxygenase subunits. The focused library was constructed using the "incorporating synthetic oligonucleotide via gene reassembly" (ISOR) method (Herman and Tawfik 2007). Briefly, ~20 μg of the α-oxygenase gene was digested using three units of DNase I (New England Biolabs Inc., USA) during 6 min at 20 °C. DNA fragments ranging between 70 and 100 bp were gel purified using a DNA isolation kit (Biological Industries, Israel) followed by ethanol precipitation. Next, 140 ng of the fragmented DNA was reassembled in the presence of 0.4 nM of the spiking oligos mixture in a 25-μl PCR reaction consisting of the following steps: 94 °C for 2 min, 94 °C for 30 s, 65 °C for 1:30 min, 62 °C for 1:30 min, 59 °C for 1:30 min, 56 °C for 1:30 min, 53 °C for 1:30 min, 50 °C for 1:30 min, 47 °C for 1:30 min, 45 °C for 1:30 min, 41 °C for 1:30 min, 72 °C for 45 s, +0.0 °C for + 0:03 min, repeat 35 times, and 72 °C for 7 min. A 1:10 dilution of the assembly PCR reaction was used as a template for a nested PCR. The PCR product was digested with *NcoI* and *EcoRI* (New England Biolabs Inc., USA) and cloned into a pETDuet vector containing the NBDO segments reductase, ferredoxin, and β-oxygenase subunits. The final libraries contained on average 2.5 ISOR mutations/gene plus 1.4 random mutations/gene. Family shuffling was done with the same method as the ISOR libraries but without the presence of spiking oligos, as described in Stemmer (1994). Eight of the selected genes together with the wild type gene were used in equal amounts for shuffling. Focused (NNK) libraries were prepared by overlap extension PCR (Reetz et al. 2008). Initially, two fragments were constructed by PCR, one fragment is at position 5′- of the targeted residue, and the other is at position 3′- to it. Each fragment was amplified with oligos containing the degenerate codon "NNK" at the targeted residue (N=nucleotides A,T,C, or G; K=nucleotides G or T). Next, the two fragments were amplified together in an overlap PCR reaction in the presence of external primers, to receive the complete gene with the NNK degeneracy at the targeted position. All PCR reactions were done using Phusion taq (New England BioLabs Inc, USA) according to the manufacturer's instructions and using a themrocycler (labcycler, SensoQuest, Göttingen, Germany). Site-directed mutagenesis

(mutagenesis to a specific residue) was done with the same method; however, the oligos contained the codon for the desired replacement instead of an NNK codon.

SDS-PAGE Expressing cells were diluted to OD_{600}~2.3. Suspension of 75 μl was diluted 3:1 with a sample buffer and loaded together with a protein marker (BLUeye prestained protein ladder, GeneDireX, Hylabs Ltd., Rehovot, Israel) onto 12 % sodium dodecyl sulfate polyacrylamide gel electrophoresis (SDS-PAGE). After electrophoresis, the gel was dyed with coomassie blue stain (Sambrook et al. 1989). Quantification of band intensity was done using ImageJ program (US National Institute of Health, Bethesda, Maryland, USA).

Analytical methods HPLC and GC-MS analyses were done as described before (Brouk et al. 2010). HPLC analysis was performed with an Agilent 1100-series instrument (Agilent Technologies, USA) using an Eclipse XDB-C_{18} column (5 μm, 4.6×150 mm; Agilent Technologies, USA) equipped with a photodiode array detector. The isocratic elution was performed with 85 % acidic H_2O (0.1 % formic acid) and 15 % acetonitrile as the mobile phase at a flow rate of 1 ml/min. Compounds were identified by comparison of retention times at 275 nm and UV-visible spectra to those of standards. Retention times were HTyr=2.4 min, 3-nitrophenyl 1,2-ethandiol—6.4 min. Samples for GC-MS were analyzed using a GC 6890N (Agilent Technologies, USA) instrument equipped with a capillary HP-5 column (30 m×0.32 mm×0.25 μm, Agilent Technologies, USA) and an HP-5975 mass spectra detector (Agilent Technologies, USA). The detection of the biotransformation products required derivatization with silyl groups. The silylation was performed by adding 200-μl N,O-bis (trimethylsilyl)-acetamide (Fluka, USA) to 400 μl of biotransformation products extracted by ethyl acetate (1:1 ratio between the biotransformation buffer and ethyl acetate). The solution was incubated at 80 °C for 20 min following evaporation under N_2 flow and resuspension in ethyl acetate. The silylated products were injected to the GC-MS with helium as carrier gas maintained at 1 ml/min. Identification was based on comparison of mass spectra and retention time with those of standards, as well as an MS library data (NIST mass spectral library V. 2.0). The GC-MS fragmentation products and relative intensity of 3-nitrophenyl 1,2-ethandiol, to which a standard does not exist, were the following: 43(9.9), 103 (15.8), 147 (65.3), 75 (11.8), 208 (62.7), 133 (11.6), 224 (51.4), and 32 (11.2). LC-MS analysis was done using an Acquity UPLC system from Waters. The chromatographic separation was achieved using the same column and conditions described above. A sample of 30 μl was injected; the flow rate of the eluent was 300 μl/min. An LCT Premier mass spectrometer from Waters Corporation (Milford, MA, USA) under ESI conditions was used for mass detection in negative mode. To purify 3-nitrophenyl 1,2-ethandiol, 10 l of culture of variant F293I which produces high amounts of this product was grown under the conditions described above. After resuspension in the biotransformation buffer with 0.5-mM 3NPA, the culture was incubated with shaking at 30 °C for 3 h. The biotransformation products were extracted by ethyl acetate (100 ml); after volume reduction by evaporation, 500 μl was loaded on a TLC plate (20×20-cm silica gel 60 F_{254}, Merck, Germany) and separated with ethyl acetate, methanol, and hexane at ratios of 1:4:5. The correct spot was scraped and purified from the TLC plate by extraction with 1-ml ethyl acetate, evaporated and resuspended in $CDCl_3$ (Sigma-Aldrich chemicals Ltd., Rehovot, Israel). Proton NMR spectroscopy was performed on Bruker Avance AV-III 400 spectrometer operating at 400.40-MHz resonance frequency (Bruker, Billerica, MA, USA). Five-millimeter outer diameter glass tubes were used with broadband (BBO) probe heads with automatic tuning equipped with *z*-gradients and 2H lock. Typical data were collected with 256 scans, a 60.8-s dwell time, and a relaxation time of 1 s. The peaks in the spectrum were identified by comparison with a predicted spectrum (ChemSketch program; Advanced Chemistry Development (ACD/labs), Toronto, Canada) and a published spectrum (Mahajabeen and Chadha 2011; Wei et al. 2000).

Molecular docking AutoDock Vina was used for docking experiments (Scripps Research Institute, La Jolla, CA, USA) (Vargas et al. 1999). In AutoDock Vina, the substrate was treated as a flexible ligand by modifying its rotatable torsion, while NBDO (PDB code 2BMR (Friemann et al. 2005)) was considered as a rigid receptor. All variants of NBDO were prepared using Chimera and PyMol (Feingersch et al. 2008). The Fe atom and two water molecules located at a distance of <4 Å from the metal are considered part of the receptor. The receptor was prepared using AutoDock tools package (Scripps Research Institute). All residues were checked to guarantee that the program assigned the correct charges to each ionizable side chain. The structures of the substrates were built using Chem3D Ultra10 (CambridgeSoft Corporation, Cambridge, MA, USA), and their energy was minimized using molecular mechanics method (MM2). Following minimization, all hydrogen atoms and Gasteiger atomic charges were added in UCSF Chimera (Resource for Biocomputing, Visualization, and Informatics University of California, CA, USA). The addition of torsions and the substrate preparations was made using AutoDock tools package (Scripps Research Institute, San Diego, CA, USA). To define the grid size and location, AutoGrid function from Autodock was implemented. The final grid box was centered at 53, 65, and 1 with dimensions of 10×12×12 and spacing of 1 Å in each dimension. The exhaustiveness was set to 200. More than 10 individual runs were made for each substrate and each variant in order to receive reliable and comparable results.

Results

Library construction and screening NBDO is a multicomplex enzyme made of four subunits which assemble a heterohexamer, a reductase, and a ferredoxin. In order to make screening more efficient, mutagenesis was carried out on the α-oxygenase subunit which is responsible for substrate binding and catalysis (Friemann et al. 2005; Wackett 2002). Two types of libraries were constructed—a neutral drift library (Amitai et al. 2007; Gupta and Tawfik 2008) and a focused library (Fig. 2). The neutral drift library was constructed by two rounds of screens for wild type activity using a colorimetric method which is able to detect the catechol (Fishman et al. 2004; Schmidt and Bornscheuer 2005) produced from nitrobenzene hydroxylation (Nishino and Spain 1995; Parales et al. 2005). In the first round, a random library was constructed with a mutation rate of 3.5 mutations per gene using error prone PCR (epPCR). Seven hundred twenty-two variants exhibiting native activity (≤WT activity) were collected from a screen of 1,900 clones. These were used as the template pool for the second random library which had on average an additional 1.4 random mutations per gene. This second library was again screened for wild type activity, and the 1,470 positives out of 4,200 clones screened composed the random library which was screened for 3NPA hydroxylation. It is assumed that by screening for WT activity, neutral mutations were accumulated, which broaden the sequence and activity potentials of the genes in the library (and their encoded enzymes) without damaging the enzyme's stability.

The second type was a focused ISOR library, in which a random combination of 18 selected positions was mutated to preselected amino acid residues (Table S1). The 18 positions were chosen based on several considerations: alignment between NBDO and ten other proteins which either share high sequence similarity or contain the helix-grip fold which composes the hydrophobic pocket (Carredano et al. 2000; Friemann et al. 2005; Iyer et al. 2001a, b), data from previous works done on NBDO and naphtalene dioxygenase (NDO) (Ferraro et al. 2006; Friemann et al. 2005; Ju and Parales 2006, 2009; Kauppi et al. 1998; Lessner et al. 2002; Parales 2003; Resnick et al. 1996), and on the HotSpot Wizard (Pavelka et al. 2009). The focused library was constructed using the ISOR method (Herman and Tawfik 2007) and contained an average of 2.5 replacements per gene plus 1.4 random mutations per gene to create a low-medium mutational load. These two approaches (neutral drift and focused libraries) are often used to create high-quality libraries enriched in nondeleterious mutations, especially when the screening method is limited to the scale of ~10^3–10^4 mutants (Dalby 2011; Gupta and Tawfik 2008).

Initially, several compounds were examined as substrates for HTyr production, 2-phenylethanol, 4-nitrophenethyl alcohol, and 3-nitrophenethyl-alcohol (3NPA). Only 3NPA was oxidized (albeit to a small extent) by NBDO, and therefore was chosen as the substrate for directed evolution. The screen for activity on 3NPA was based on a colorimetric method which detects NO_2 release from the substrate as a result of its hydroxylation (Ju and Parales 2006). The initial activity of the wild type measured by this assay was 0.05 nmol min^{-1} mg $protein^{-1}$. The error-prone enriched library (1,470 variants) and the focused library (3,000 variants) were screened using this method.

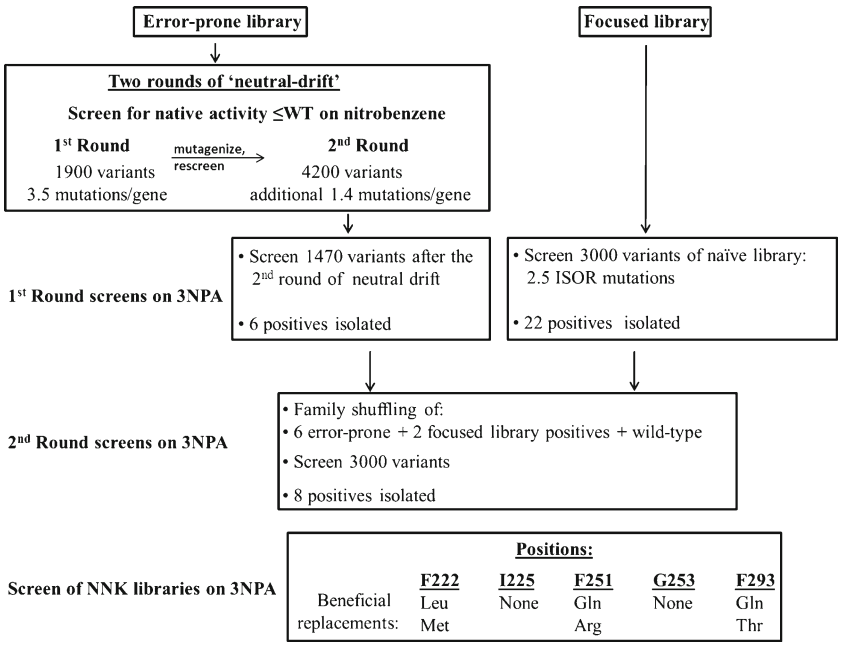

Fig. 2 A scheme describing the screening and selections performed in this study. Initially, two types of libraries were screened seperately for activity on 3NPA, a neutral drift library and a focused library. The best variants of each were shuffled together with wild type and screened for activity on 3NPA. Mutations from the best variants from the second round of screening convereged to five dominant poitions. Saturation mutagenesis (NNK) libraries were prepared for each of these positions and screened for activity on 3NPA to identify the best replacements at these positions

The first round of screening produced six improved variants, which originated from the error-prone library. Position F293 was the most dominant although the variability of these mutants was quite high. These variants were further characterized and were the basis for the second round of screening. The ISOR library screened on 3NPA showed 9.4 % positives which were defined as variants with the same or better activity than wild type. Twenty-two of the most promising variants were sequenced. These variants were threefold to fivefold better than wild type in the screen, and indeed, the sequence showed convergence to mutations in three main positions (251, 253, 293; data not shown).

For the second round of screening on 3NPA, a new library was constructed by shuffling six variants of the error-prone library, two of the focused library and wild type genes at equal ratios (Fig. 2, Table S2). Out of 3,000 clones from this shuffled library, the best eight—those that showed the highest activity in the screen and had a unique sequence—were isolated and characterized by kinetic measurements. In order to rule out the effect of different translation levels on activity, we verified that all mutants have similar translation levels by quantifying the bands corresponding to the α-oxygenase from an SDS-PAGE gel (Figure S1).

Improved variants by screening libraries of site-specific mutagenesis The activity of variants selected from the second round (shuffled library) was improved drastically (up to 375-fold better than wild type in variant F222C/F251L/G253D, Table 1). This increase in activity can be attributed to the elimination of satellite mutations (deleterious mutations which appeared randomly together with the beneficial mutations), on one hand, and a combination of mutations which have positive synergism within a single variant, on the other hand.

The variants can be roughly divided in two groups based on their nitrite release activity. The higher-activity group contained the three mutations F222C/F251L/G253D (250–375-fold better activity than wild type). The second less active group contained the mutation F293Q (104–150-fold better activity than wild type). Together, these mutations converged into four main positions: F222, F251, G253, and F293. In order to learn more about the role of each position and to find possible replacements in addition to those determined by the focused and error-prone libraries, we screened saturation mutagenesis libraries at each of these positions individually (NNK libraries in which N=A,C,G,T and K=T,G nucleotides). Only positions F222, F293, and F251 produced variants, which were significantly better than wild type with the following replacements: F293Q/T, F222M/L, F251R/Q. These replacements were examined individually and in combination. Initially, a combination of positions F222M/L and F251R were created, and then, the mutation F293Q was added. We found that on its own, each mutation is beneficial, but the combination of the mutations is critical. For example, while the combination F222M/F251R gave an additive effect, the rest of the combinations (F222M/F251Q, F222L/F251R, F222L/F251Q, and F222C/F251L) showed a positive synergistic effect to different extent (Table 1). It is interesting that the best combination resulted from replacements, which appeared initially in our screens (F222C/F251L).

An attempt was made to create a superior mutant by adding the beneficial mutation F293Q to other highly active mutants. Surprisingly though, when we added F293Q to the combination F222L/F251Q, as well as to our best mutant, F222C/F251L/G253D, it had a deleterious effect (activity dropped by 93.5- and 7-fold, respectively, Table 1). The negative effect between these positions may explain the division into two groups of mutants (F222/F251/G253 vs F293), which we obtained in our screens. Molecular docking with the AutoDock Vina (Morris et al. 2009; Trott and Olson 2010) was used to further learn about the influence of beneficial mutations. The criteria for the docking model were low binding energy as well as ~5 Å distance between the catalytic iron and its target on the substrate, which is common among this family of enzymes (Lipscomb 2008; Resnick et al. 1995; Seo et al. 2010; Yu et al. 2001). When comparing the docking of the substrate, 3NPA, in the mutants to the wild type, it is very clear that 3NPA is aligned correctly in the mutants but not in the wild type, i.e., the nitro group is facing N258 and the aromatic ring is close to the catalytic Fe atom (Fig. 3). In each of the improved mutants, F293Q and F222C/F251L/D253G, the docking revealed that the mutations vacate extra space for the larger substrate. In mutant F293Q, in addition to the extra space, there are potential hydrogen bonds available between the substrate and 293Q which position it slightly different than in the mutant F222C/F251L/D253G (Fig. 3). The docking model of the combined mutant, F222C/F251L/D253G/F293Q, reveals that the mutated residues C222 and Q293 are very close to one another within the active site (the sulfur atom of C222 is at a hydrogen bond distance from Q293's oxygen and nitrogen atoms); this might lead to reduced affinity of the substrate to Q293. The activity toward the native substrate, NB, was measured for selected mutants and was found to decrease in all of them compared with wild type (Table 1). Additionally, no novel activity of the best mutant was detected toward 2-phenylethanol or 4-nitrophenethyl alcohol, leading to the conclusion that the mutants evolved specifically to fit 3NPA. Our trial at rationally combining beneficial mutations failed; however, screening random combinations succeeded. In the second round, we received the mutant S224P/F251L/G253D/F293I, this mutant combines mutations at positions 251, 253, and 293. On its own, mutation F293I is inferior to F293Q; however, in combination with F251L and G253D, it is superior to it with activity ~238-fold better than wild type and with almost undetectable side product formation.

Table 1 Activity of evolved and engineered mutants on the substrate 3NPA

Variant	Origin of variant	NO_2 release from 3NPA[a] (nmol min^{-1} mg $protein^{-1}$)	Side product[b] (% of HTyr peak)	NO_2 release from NB[a] (nmol min^{-1} mg $protein^{-1}$)
WT	–	0.05±0.00	177	9.27±0.29
F293T	NNK and focused libraries	5.5±0.80	20	
F293Q	NNK and focused libraries	5.3±2.00	0	2.10±0.33
F222M	NNK library	1.13±0.04	21.2	
F222L	NNK library	1.21±0.12	15	
F251Q	NNK and focused libraries	0.6±0.00	350	
F251R	NNK and focused libraries	0.36±0.09	139	
F222M/F251R	Engineered mutant	1.26±0.18	62.9	
F222M/F251Q	Engineered mutant	4.98±0.15	25.8	
F222L/F251R	Engineered mutant	3.30±0.01	35.7	
F222L/F251Q	Engineered mutant	9.83±1.45	13.5	3.46±0.78
F222L/F251Q/F293Q	Engineered mutant	0.106±0.84	346	
F222L/F251Q/G253D	Engineered mutant	3.33±0.04	8.03	
F222C/F251L/G253D	Family shuffling	18.78±0.06	7.7	6.26±0.95
F222C/F251L	Engineered mutant	8.96±0.50	11.2	3.07±0.57
F222C/F251L/G253D/F293Q	Engineered mutant	2.88±0.20	107	

[a] The standard deviation is an average of three repeats. These values were measured from the NO_2 release rate, and therefore represent production of HTyr (3NPA substrate) or catechol (NB substrate) only. All measurements were done using whole cells

[b] The side product, 3-nitrophenyl-1,2-ethanediol, is not commercially available and was not quantified; therefore, in order to compare the level of its production between the mutants, the HPLC peak area of the side product was calculated as percentage of the HTyr at a single time point (1 h)

Screening of NNK libraries at position G253 did not show significant increase in activity over wild type, and indeed, sequence analysis of five variants which appeared positive in the screen contained wild type sequence. This might indicate that either this position is neutral on its own or that it is beneficial only in combination with other mutations. Because the mutation G253D appeared in our best mutant, we further examined its role despite its apparent neutrality. For this purpose, we created the mutants F222L/F251Q/G253D and F222C/F251L. When adding the mutation G253D to the combination F222L/F251Q, there was a ~3-fold decrease in activity; however, when adding it to the combination F222C/F251L, there was an ~2-fold increase in activity, both toward 3NPA and NB (Table 1). It appears that this position has different influence depending on its surroundings. On its own, it is neutral or even slightly deleterious (based on results from the NNK library at this position), but it can be either deleterious or advantageous, according to its neighboring residues.

Product selectivity of the evolved variants In addition to the nitrite release measurements, the biotransformation products were analyzed by HPLC and GC-MS. Some of the mutants produced another side-product (Table 1). The additional product was identified as 3-nitrophenyl 1,2-ethanediol (Fig. 1) by LC-MS and NMR (Figures S2 and S3). In our mutants, the formation of this additional oxidation product was greatly affected by the mutations' position and type. For example, a replacement of F293 to either Gln or Thr reduced this side activity whereas a replacement to Ile or Leu increased it. The combination of two mutants: F222L/F251Q with F293Q created a mutant with high production of the side product despite the fact that each of them on its own produced negligible amount of the side product (Table 1). The same effect was shown in a work also on NBDO, in which the type of mutation at the same position led to a different product profile (Ju and Parales 2006). The best mutants isolated in this study (F293Q and F222C/F251L/G253D) have negligible production of side products probably due to the correct and strong binding of the substrate 3NPA in the active site, a property which probably contributes to their high activity.

Discussion

In this work, several protein engineering techniques have been employed in order to engineer NBDO for the production of the antioxidant HTyr using whole cell catalysis. Four types of libraries were prepared, the first is a "neutral drift" library in which an error-prone library was enriched in potentially beneficial mutations by two rounds of screening for wild type activity. The second is a "focused library" in which only selected residues were mutated to specific amino acids based

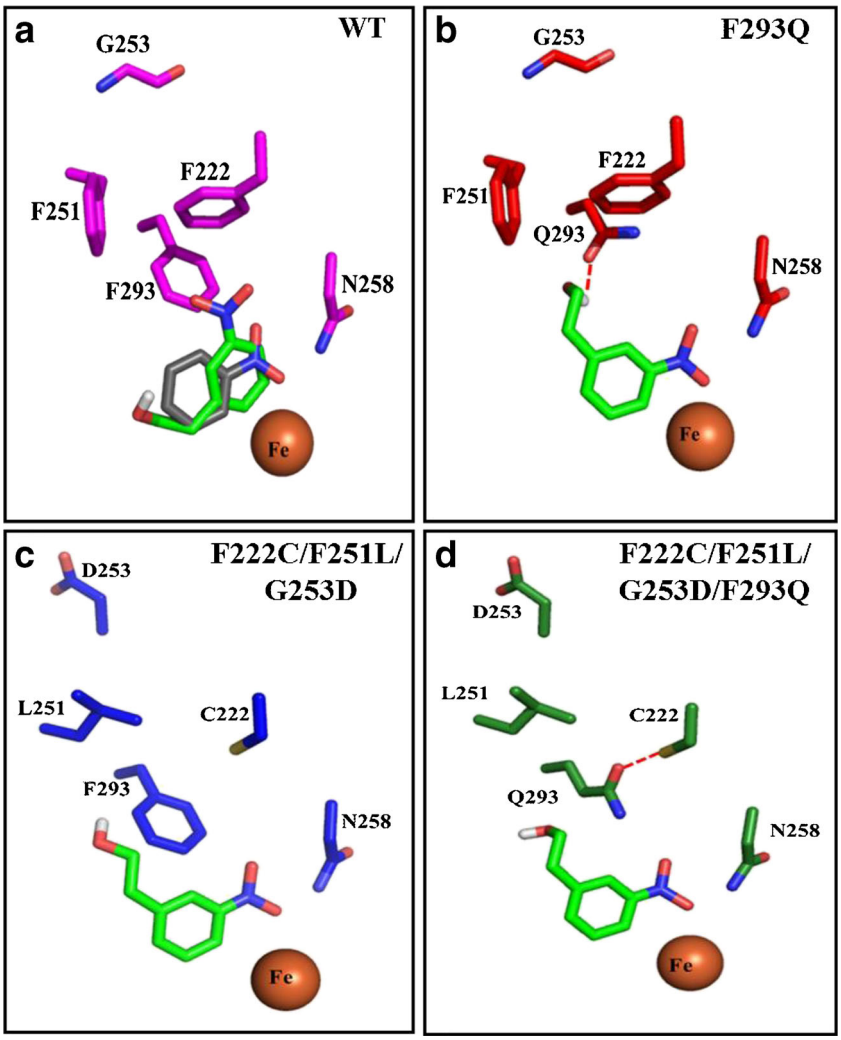

Fig. 3 Docking of 3NPA within active site of wild type NBDO and selected variants. The substrate, 3NPA (*green sticks*) was docked into wild type (**a**), the best two variants, F293Q (**b**) and F222C/F251L/G253D (**c**), as well as into the combined mutant F222C/F251L/G253D/F293Q (**d**). The residues which were mutated and the conserved N258 are shown in sticks. The catalytic Fe atom is shown as an *orange sphere*. Docking was predicted by AutoDock Vina based on NBDO's crystal structure with the substrate 3-nitrotoluene (PDB code 2BMR). Potential hydrogen bonds are shown as a *dashed red line*. For comparison, the location of the native substrate, NB, is shown in the WT structure as *grey sticks* (**a**). (Color figure online)

on previous work, phylogenetic analysis, and the "HotSpot" server. The third library was produced from shuffling of positive variants, which were found in the neutral drift and focused libraries, and finally a saturation mutagenesis library in positions which were identified from screening of the libraries described above. Combining several engineering approaches often leads to superior results (Dror and Fishman 2012). At the end of the process, four influential positions were identified; three are within the active site pocket (positions F222, F251, F293) and another in a flexible loop close to the active site (position G253). Only two positions (F251 and F293) were previously reported to affect substrate selectivity, of which F293 was actually mutated and was found to modulate substrate specificity due to its close interaction with the substrate (Friemann et al. 2005; Ju and Parales 2006; Lessner et al. 2002). In the work of Ju and Parales (2006), the mutations F293Q/I have different effects on NBDO's activity toward various substrates that were tested. For example, the products from the substrate 4-nitrotoluene were preferentially 4-methylcatechol (oxidation of the aromatic ring) in the F293I mutant but 4-nitrobenzyl alcohol (oxidation of the alkyl chain) in the F293Q mutant. The products from the substrate 3-nitrotoluene were the same in the two mutants. Here, as well, while 3NPA oxidation is improved by several possible replacements in this position, only one replacement (F293Q) is ideal in terms of specific activity. Position F222 was identified as one of the residues which line the active site (Friemann et al. 2005); however due to its conservation, it was not considered for purposes of protein engineering (despite its identification by the "HotSpot Wizard" server as one). Nevertheless, this position was selected from the neutral drift (error prone) library and has a very strong positive effect on 3NPA oxidation. Another position which was selected is G253. This residue is not lining the active site nor was it identified by the "HotSpot Wizard" server. Nevertheless, despite its apparent neutrality, it is an essential participant in the triple mutant (F222C/F251L/G253D) which has the highest 3NPA oxidation activity (Table 1). The role of mutation G253D is not clear. Mutation G253D presents a new negative charge which is facing the hydrophilic solvent and might help

in the enzyme's solubility, since when overexpressed, it is prone to aggregate (SDS-PAGE analysis, Figure S1). Another possibility is a structural role affecting a loop which constitutes a "gate" to the active site (Parales et al. 2005). The G253D mutation originated from the focused library and represents a consensus residue in a loop close to the active site. Such consensus mutations are known to increase stability (Dalby 2011). A similar effect was described before for an oxidizing enzyme; a stabilized mutant of cytochrome P450 could acquire new activities by beneficial but destabilizing mutations (Bloom et al. 2006). Despite its apparent neutrality and positive synergistic effect in the best variant F222C/F251L/G253D/, mutation G253D is not always favorable in combination with other beneficial mutations. For example, when it is combined with the successful mutations 222L/251Q, it has a negative effect on activity. A similar effect was found in the enzyme 2-nitrotoluene dioxygenase (2NTDO), which acquired three mutations in order to allow growth on 4-nitrotoluene as a carbon source. One of the triple mutations is beneficial only when it appears with one of the other two; on its own, it is deleterious (Ju and Parales 2011). Such complexity in the evolution trajectory leading to the best solution enhances the importance of random screens.

Docking of the substrate within the active sites of the various mutants and wild type revealed the reason for the increased activity: The substrate within the mutants is well-aligned and anchored in its productive form, meaning, the nitro group facing N258 and the aromatic ring well oriented in respect to the catalytic Fe atom. Indeed, many oxygenases acquire new activities by accommodating their active site to the new substrate without changing the catalytic mechanism (Ferraro et al. 2006; Seo et al. 2010). As the chemistry of the oxidation does not change, it is the orientation of the substrate within the active site that determines at which carbon atom oxidation occurs. Some of our mutants are able to oxidize the substrate on the alkyl moiety without removal of the nitro group. Because the various mutations affect the positioning of the substrate within the active site, their ability to oxidize a second site is variable. It is known that in this family of enzymes, the production of several products is also a function of the positioning of the substrate within the binding pocket, which is determined by the nature of the substrate and the residues which bind to it (Boyd et al. 2001; Carredano et al. 2000; Seo et al. 2010; Yu et al. 2001). For example, a study done on the regioselectivity of NDO showed that the substrate phenantrene is positioned differently in wild type and a mutant such that the product is dictated by which carbon on the ring is closest to the oxidizing Fe atom. Similarly, in the same study, the substrate 3-nitrotoluene is hydroxylated on its alkyl chain by wild type NDO due to its positioning in the active site close to the oxidizing Fe atom (Ferraro et al. 2006). Oxidation of the alkyl moiety, by NBDO, has been observed before (Ju and Parales 2006, 2009; Lessner et al. 2002).

At the end of the selections, we have obtained a mutant which is 375-fold better than wild type in 3NPA oxidation with a specific activity rate of 18.8 nmol min^{-1} mg $protein^{-1}$ (Table 1, corresponding approximately 36.6 μmol min^{-1} g_{dcw}^{-1}). This value is an underestimation since the process was not optimized and glucose was not present in the whole cell biotransformation to facilitate NADH regeneration. In comparison, *E. coli* cells harboring toluene 4-monooxygenase variant I100A/E214G/D285Q, which was engineered to produce HTyr from 2-phenylethanol, had an initial specific activity of 4.4 nmol min^{-1} mg $protein^{-1}$ which was further improved to 160 nmol min^{-1} mg $protein^{-1}$ following optimization of growth and biotransformation conditions on 1-l scale (Brouk and Fishman 2012). Grant et al. (2011) recently reported production rates for the conversion of n-dodecane to the corresponding alcohol and acid by *E. coli* cells expressing the alkane-1-monoxygenase (alkB) complex of *Pseudomonas putida* GPo1. The maximum specific activity for the combined alcohol and acid in a two-phase bioreactor (2-l scale) was 3.5 μmol min^{-1} g_{dcw}^{-1}, which is tenfold lower than the potential specific activity of NBDO variant F222C/F251L/G253D. Nonetheless, the volumetric productivity was 0.35 g l^{-1} h^{-1} (total volume of both phases). Although process engineering was beyond the scope of this work, presently, 10 l of culture at OD_{600}=10 yielded 1.21-g HTyr within an hour, indicating a productivity of 0.12 g l^{-1} h^{-1}. This achievement is notable both in terms of protein engineering and synthesis of HTyr, which at the moment is produced at a yield of 1.225 g from 1 l of waste water (Allouche et al. 2003).

Acknowledgments We would like to thank Onit Alalouf and Dr. Yael Balazs for their help in NMR data analysis and Larissa Panz for her help with LC-MS data analysis.

References

Allouche N, Sayadi S (2005) Synthesis of hydroxytyrosol, 2-hydroxyphenylacetic acid, and 3-hydroxyphenylacetic acid by differential conversion of tyrosol isomers using *Serratia marcescens* strain. J Agric Food Chem 53(16):6525–6530

Allouche N, Fki I, Sayadi S (2003) Toward a high yield recovery of antioxidants and purified hydroxytyrosol from olive mill wastewaters. J Agric Food Chem 52(2):267–273

Allouche N, Damak M, Ellouz R, Sayadi S (2004) Use of whole cells of *Pseudomonas aeruginosa* for synthesis of the antioxidant hydroxytyrosol via conversion of tyrosol. Appl Environ Microbiol 70(4):2105–2109

Amitai G, Gupta RD, Tawfik DS (2007) Latent evolutionary potentials under the neutral mutational drift of an enzyme. HFSP J 1(1):67–78

Bloom JD, Labthavikul ST, Otey CR, Arnold FH (2006) Protein stability promotes evolvability. Proc Natl Acad Sci U S A 103(15):5869–5874

Bouallagui Z, Bouaziz M, Lassoued S, Engasser JM, Ghoul M, Sayadi S (2011) Hydroxytyrosol acyl esters: biosynthesis and activities. Appl Biochem Biotechnol 163(5):592–599

Boyd DR, Sharma ND, Allen CC (2001) Aromatic dioxygenases: molecular biocatalysis and applications. Curr Opin Biotechnol 12(6): 564–573

Bradford MM (1976) A rapid and sensitive method for the quantitation of microgram quantities of protein utilizing the principle of protein-dye binding. Anal Biochem 72:248–254

Brouk M, Fishman A (2009) Protein engineering of toluene monooxygenases for synthesis of hydroxytyrosol. Food Chem 116:114–121

Brouk M, Fishman A (2012) Improving process conditions of hydroxytyrosol synthesis by toluene-4-monooxygenase. J Mol Catal B Enzym 84:121–127

Brouk M, Nov Y, Fishman A (2010) Improving biocatalyst performance by integrating statistical methods into protein engineering. Appl Environ Microbiol 76(19):6397–6403

Carredano E, Karlsson A, Kauppi B, Choudhury D, Parales RE, Parales JV, Lee K, Gibson DT, Eklund H, Ramaswamy S (2000) Substrate binding site of naphthalene 1,2-dioxygenase: functional implications of indole binding. J Mol Biol 296(2):701–712

Cicerale S, Lucas L, Keast R (2012) Antimicrobial, antioxidant and anti-inflammatory phenolic activities in extra virgin olive oil. Curr Opin Biotechnol 23(2):129–135

Dalby PA (2011) Strategy and success for the directed evolution of enzymes. Curr Opin Struct Biol 21(4):473–480

Dror A, Fishman A (2012) Engineering non-heme mono- and dioxygenases for biocatalysis. Comput Struct Biotechnol J 2(3):1–12

Espin JC, Soler-Rivas C, Cantos E, Tomas-Barberan FA, Wichers HJ (2001) Synthesis of the antioxidant hydroxytyrosol using tyrosinase as biocatalyst. J Agric Food Chem 49(3):1187–1193

Feingersch R, Shainsky J, Wood TK, Fishman A (2008) Protein engineering of toluene monooxygenases for synthesis of chiral sulfoxides. Appl Environ Microbiol 74(5):1555–1566

Ferraro DJ, Okerlund AL, Mowers JC, Ramaswamy S (2006) Structural basis for regioselectivity and stereoselectivity of product formation by naphthalene 1,2-dioxygenase. J Bacteriol 188(19):6986–6994

Fishman A, Tao Y, Bentley WE, Wood TK (2004) Protein engineering of toluene 4-monooxygenase of *Pseudomonas mendocina* KR1 for synthesizing 4-nitrocatechol from nitrobenzene. Biotechnol Bioeng 87(6):779–790

Friemann R, Ivkovic-Jensen MM, Lessner DJ, Yu CL, Gibson DT, Parales RE, Eklund H, Ramaswamy S (2005) Structural insight into the dioxygenation of nitroarene compounds: the crystal structure of nitrobenzene dioxygenase. J Mol Biol 348(5):1139–1151

Fuchs G, Boll M, Heider J (2011) Microbial degradation of aromatic compounds—from one strategy to four. Nat Rev Microbiol 9(11): 803–816

Grant C, Woodley JM, Baganz F (2011) Whole-cell bio-oxidation of n-dodecane using the alkane hydroxylase system of *P. putida* GPo1 expressed in *E. coli*. Enzyme Microb Technol 48(6–7):480–486

Gupta RD, Tawfik DS (2008) Directed enzyme evolution via small and effective neutral drift libraries. Nat Methods 5(11):939–942

Herman A, Tawfik DS (2007) Incorporating synthetic oligonucleotides via gene reassembly (ISOR): a versatile tool for generating targeted libraries. Protein Eng Des Sel 20(5):219–226

Iyer LM, Aravind L, Koonin EV (2001a) Common origin of four diverse families of large eukaryotic DNA viruses. J Virol 75(23):11720–11734

Iyer LM, Koonin EV, Aravind L (2001b) Adaptations of the helix-grip fold for ligand binding and catalysis in the START domain superfamily. Proteins 43(2):134–144

Ju KS, Parales RE (2006) Control of substrate specificity by active-site residues in nitrobenzene dioxygenase. Appl Environ Microbiol 72(3):1817–1824

Ju KS, Parales RE (2009) Application of nitroarene dioxygenases in the design of novel strains that degrade chloronitrobenzenes. Microb Biotechnol 2(2):241–252

Ju KS, Parales RE (2011) Evolution of a new bacterial pathway for 4-nitrotoluene degradation. Mol Microbiol 82(2):1365–2958

Kauppi B, Lee K, Carredano E, Parales RE, Gibson DT, Eklund H, Ramaswamy S (1998) Structure of an aromatic-ring-hydroxylating dioxygenase-naphthalene 1,2-dioxygenase. Structure 6(5):571–586

Kovaleva EG, Lipscomb JD (2008) Versatility of biological non-heme Fe(II) centers in oxygen activation reactions. Nat Chem Biol 4(3): 186–193

Lessner DJ, Johnson GR, Parales RE, Spain JC, Gibson DT (2002) Molecular characterization and substrate specificity of nitrobenzene dioxygenase from *Comamonas* sp. strain JS765. Appl Environ Microbiol 68(2):634–641

Lipscomb JD (2008) Mechanism of extradiol aromatic ring-cleaving dioxygenases. Curr Opin Struct Biol 18(6):644–649

Mahajabeen P, Chadha A (2011) One-pot synthesis of enantiomerically pure 1, 2-diols: asymmetric reduction of aromatic α-oxoaldehydes catalysed by *Candida parapsilosis* ATCC 7330. Tetrahedron Asymmetry 22(24):2156–2160

Morris GM, Huey R, Lindstrom W, Sanner MF, Belew RK, Goodsell DS, Olson AJ (2009) AutoDock4 and AutoDockTools4: automated docking with selective receptor flexibility. J Comput Chem 30(16): 2785–2791

Nishino SF, Spain JC (1995) Oxidative pathway for the biodegradation of nitrobenzene by *Comamonas* sp. strain JS765. Appl Environ Microbiol 61(6):2308–2313

Parales RE (2003) The role of active-site residues in naphthalene dioxygenase. J Ind Microbiol Biotechnol 30(5):271–278

Parales RE, Huang R, Yu CL, Parales JV, Lee FK, Lessner DJ, Ivkovic-Jensen MM, Liu W, Friemann R, Ramaswamy S, Gibson DT (2005) Purification, characterization, and crystallization of the components of the nitrobenzene and 2-nitrotoluene dioxygenase enzyme systems. Appl Environ Microbiol 71(7):3806–3814

Pavelka A, Chovancova E, Damborsky J (2009) HotSpot Wizard: a web server for identification of hot spots in protein engineering. Nucleic Acids Res 37(Web Server issue):376–383

Reetz MT, Kahakeaw D, Lohmer R (2008) Addressing the numbers problem in directed evolution. Chembiochem 9(11):1797–1804

Resnick SM, Torok DS, Lee K, Brand JM, Gibson DT (1995) Regiospecific and stereoselective hydroxylation of 1-indanone and 2-indanone by naphthalene dioxygenase and toluene dioxygenase. Appl Environ Microbiol 61(2):847

Resnick SM, Lee K, Gibson DT (1996) Diverse reactions catalyzed by naphthalene dioxygenase from *Pseudomonas* sp. strain NCIB 9816. J Ind Microbiol Biotechnol 17(5):438–457

Sambrook J, Fritsch E, Maniatis T (1989) Molecular cloning: a laboratory manual, vol 2, 2nd edn. Cold Spring Harbor, NY

Satoh Y, Tajima K, Munekata M, Keasling JD, Lee TS (2012) Engineering of l-tyrosine oxidation in *Escherichia coli* and microbial production of hydroxytyrosol. Metab Eng 14(6):603–610

Schmidt M, Bornscheuer UT (2005) High-throughput assays for lipases and esterases. Biomol Eng 22(1–3):51–56

Seo J, Kang SI, Ryu JY, Lee YJ, Park KD, Kim M, Won D, Park HY, Ahn JH, Chong Y, Kanaly RA, Han J, Hur HG (2010) Location of flavone B-ring controls regioselectivity and stereoselectivity of naphthalene dioxygenase from *Pseudomonas* sp. strain NCIB 9816–4. Appl Microbiol Biotechnol 86(5):1451–1462

Shainsky J, Bernath-Levin K, Isaschar-Ovdat S, Glaser F, Fishman A (2013) Protein engineering of nirobenzene dioxygenase for enantioselective synthesis of chiral sulfoxides. Protein Eng Des Sel 26(5):335–345

Stemmer WP (1994) DNA shuffling by random fragmentation and reassembly: *in vitro* recombination for molecular evolution. Proc Natl Acad Sci U S A 91(22):10747–10751

Trott O, Olson AJ (2010) AutoDock Vina: improving the speed and accuracy of docking with a new scoring function, efficient optimization, and multithreading. J Comput Chem 31(2):455–461

Vargas RR, Bechara EJH, Marzorati L, Wladislaw B (1999) Asymmetric sulfoxidation of a beta-carbonyl sulfide series by chloroperoxidase. Tetrahedron Asymmetry 10(16):3219–3227

Wackett LP (2002) Mechanism and applications of Rieske non-heme iron dioxygenases. Enzyme Microb Technol 31:577–587

Wei ZL, Lin GQ, Li ZY (2000) Microbial transformation of 2-hydroxy and 2-acetoxy ketones with *Geotrichum* sp. Bioorg Med Chem 8(5): 1129–1137

Yu CL, Parales RE, Gibson DT (2001) Multiple mutations at the active site of naphthalene dioxygenase affect regioselectivity and enantioselectivity. J Ind Microbiol Biotechnol 27(2):94–103